PALEOCEANOGRAPHY, VOL. 29, 1–12, doi:10.1002/2012PA002448, 2014

Surface water conditions and calcium carbonate preservation in the Fram Strait during marine isotope stage 2, 28.8–15.4 kyr

K. Zamelczyk,[1,2] T. L. Rasmussen,[1] K. Husum,[2] F. Godtliebsen,[3] and M. Hald[2]

Received 20 December 2012; revised 20 October 2013; accepted 18 November 2013; published 14 January 2014.

[1] We present a high-resolution record of calcium carbonate preservation alongside the distribution pattern of planktic foraminifera from the Fram Strait. The record covers the marine isotope stage (MIS) 2, 28.8 to 15.4 kyr, including the Last Glacial Maximum (LGM) and the early deglaciation in multidecadal temporal resolution. The investigation is based on the distribution patterns of planktic foraminifera, stable isotopes, mean shell weight of *Neogloboquadrina pachyderma*, the degree of fragmentation of planktic shells, $CaCO_3$ content, and geochemical and sedimentological data. The dissolution proxies indicate long-lasting periods of markedly reduced preservation of calcium carbonate at ~28.8–27.2, ~24.1–23.2, and ~16.6–15.4 kyr in addition to a number of short-lasting periods (< 300 year) during the LGM. These periods are accompanied by a simultaneous and significant reduction in specimens of subpolar planktic foraminifera indicating a southward expansion of Arctic surface water masses. Prolonged periods with high abundances of subpolar foraminiferal species and good preservation of calcium carbonate are attributed to increased influence of Atlantic water masses, which appears to persist throughout most of the MIS 2. Comparison to Holocene (MIS 1) shell weight records shows that the preservation during MIS 2 was overall better, even during the events of dissolution. This was probably a reflection of the low concentration of atmospheric CO_2 at the time.

Citation: Zamelczyk, K., T. L. Rasmussen, K. Husum, F. Godtliebsen, and M. Hald (2014), Surface water conditions and calcium carbonate preservation in the Fram Strait during marine isotope stage 2, 28.8–15.4 kyr, *Paleoceanography*, *29*, 1–12, doi:10.1002/2012PA002448.

1. Introduction

[2] During MIS 2 the sea-surface conditions in the Nordic Seas and the Fram Strait were highly variable. This was attributed to changes in the advection of Atlantic water masses to high latitudes [*Hebbeln et al*., 1994]. The inflow of the relatively warm and saline Atlantic water masses generated seasonally ice free conditions but at the same time caused instability of the Svalbard-Barents Sea ice sheet and episodic release of meltwater [*Hebbeln et al*., 1994, 1998; *Dokken and Hald*, 1996; *Hebbeln and Wefer*, 1997; *Knies and Stein*, 1998; *Knies et al*., 1999; *Hald et al*., 2001; *Nørgaard-Pedersen et al*., 2003; *Wollenburg et al*., 2004; *de Vernal et al*., 2006; *Rasmussen et al*., 2007; *Müller et al*., 2009; *Stanford et al*., 2011]. During summer seasons, light- and high-nutrient availability resulted in high primary production at the marginal ice zones (MIZs) [*Hebbeln et al*., 1998, and references herein]. Numerous studies on glacial-interglacial cycles indicate that the glacial sea surface water had a higher pH and a higher carbonate ion (CO_3^{2-}) concentration compared with interglacial surface water [*Sanyal et al*., 1995; *Hönisch and Hemming*, 2005; *Foster*, 2008]. These two parameters are important for calcifying planktic foraminifera [*Bijma et al*., 1999, 2002], which are significant contributors to the total production of inorganic carbon at the surface and to carbonates accumulated in marine sediments [*Schiebel*, 2002; *Schiebel et al*., 2007; *Langer*, 2008]. The proportion of calcium carbonate in the sediments is determined, among other components, by the balance between the production of calcium carbonate at the sea surface and dissolution in the water column and/or at the sea floor [*Catubig et al*., 1998]. The deposition rate of carbonates is several times lower than the production rate at the surface showing that dissolution plays an important role for the preservation of calcium carbonate. At present, planktic foraminifera are one of the most extensively used proxies for paleoceanographic reconstructions of the late Quaternary [*Hemleben et al*., 1989]. However, their calcareous shells are vulnerable to dissolution, which can modify the primary chemical properties recorded in their shells. Since certain species of planktic foraminifera are more susceptible to dissolution than other, dissolution additionally may alter the composition of the faunal assemblages and cause bias in the interpretation of the paleoenvironment and properties of past water masses.

[1]CAGE-Centre for Arctic Gas Hydrate, Environment and Climate, UiT, the Arctic University of Norway, Tromsø, Norway.
[2]Department of Geology, UiT, the Arctic University of Norway, Tromsø, Norway.
[3]Department of Mathematics and Statistics, UiT, the Arctic University of Norway, Tromsø, Norway.

Corresponding author: K. Zamelczyk, Department of Geology, University of Tromsø, Dramsveien 201 NO-9037 Tromsø, Norway. (katarzyna.zamelczyk@uit.no)

0883-8305/14/10.1002/2012PA002448

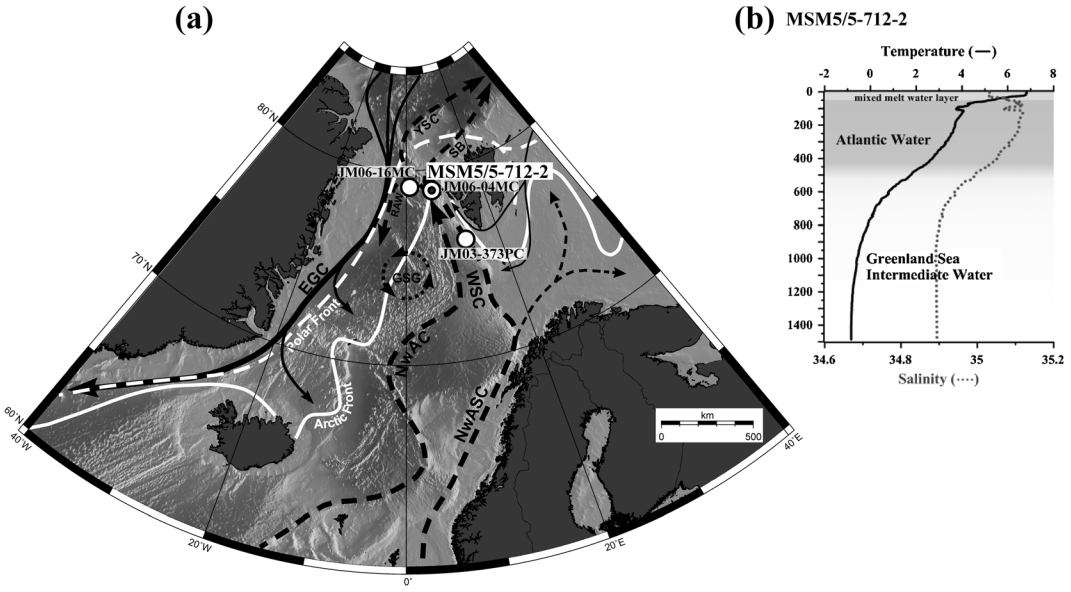

Figure 1. (a) Map of northeastern North Atlantic Ocean and the Fram Strait showing present-day surface currents and average position of the Polar and Arctic fronts (based on *Marnela et al*. [2008]). Location of core MSM (double circle) and other records mentioned in the text is indicated. Abbreviations: NwAC: Norwegian Atlantic Current; NwASC: Norwegian Atlantic Slope Current; WSC: West Spitsbergen Current; SB: Svalbard Branch; YSC: Yermak Slope Current; RAW: Recirculating Atlantic Water; EGC: East Greenland Current; GSG: Greenland Sea Gyre. (b) CTD (conductivity-temperature-depth) data of temperature and salinity from the coring site MSM5/5-712-2 taken in July 2012.

[3] Numerous studies from the Fram Strait area interpret low abundances of subpolar species and the dominance of the polar *N. pachyderma* as an indication for cold surface water conditions linked to the southward expansion of polar water masses [*Hebbeln et al*., 1994, 1998; *Dokken and Hald*, 1996; *Hebbeln and Wefer*, 1997; *Hald et al*., 2001; *Rasmussen et al*., 2007]. In addition, low temperatures are calculated using transfer functions, a statistic estimate based on changes in species composition of the faunas [e.g., *Sarnthein et al*., 2003; *Weinelt et al*., 2003]. However, recent studies of the Holocene from the Fram Strait have shown that calcite dissolution during cold periods may complicate paleoenvironmental reconstructions based on planktic foraminifera [*Zamelczyk et al*., 2012, 2013]. It is therefore important to assess the state of preservation of planktic foraminifera to obtain a better understanding of changes in surface water conditions and factors controlling the foraminiferal paleorecord in the glacial northern North Atlantic Ocean.

[4] We investigate core MSM5/5-712-2 from the western Svalbard margin situated below the northward flowing Atlantic surface water (Figure 1a). The purpose is to detect and study the effects of dissolution on the planktic foraminifera fauna and provide new details of paleoceanographic changes and carbonate preservation during the MIS 2 interval in high temporal resolution. The investigation is based on the distribution patterns of planktic foraminifera faunas, their degree of fragmentation and the mean shell weight of *N. pachyderma*, ice-rafted debris (IRD), stable isotopes, and other geochemical proxies.

2. Modern Oceanic Setting

[5] The Atlantic water masses in the Nordic Seas are divided into two branches, the Norwegian Atlantic Slope Current (NwASC) and the Norwegian Atlantic Current (NwAC) [*Walczowski et al*., 2005] (Figure 1a). In the eastern Fram Strait, these warm and saline Atlantic waters continue as the West Spitsbergen Current. North of Svalbard the advected water masses split into the subsurface Yermark Slope Current (YSC) and the Svalbard Branch (SB) (Figure 1a) [*Manley*, 1995]. In the western Fram Strait, cold, low-salinity, and ice-loaded Polar water is transported by the East Greenland Current (EGC) from the Arctic Ocean along the continental slope of Greenland. In the central Fram Strait, the two different surface water masses mix and generate Arctic water [*Hop et al*., 2006]. The extent of sea ice cover is controlled by the WSC and EGC, which also define the geographic position of the Polar front and the Arctic front and the MIZ. The average summer sea ice margin is constrained by the Polar front and the maximum limit of sea ice margin in winter by the Arctic front [*Vinje*, 1977]. The upper 100 m of the water column at the core site is characterized by a surface layer influenced by melt water overlaying a thick layer of Atlantic water (Figure 1b). Greenland Sea intermediate water produced by deep convection of Atlantic water in the Greenland Sea is found below ~500 m water depth (Figure 1b) [*Swift and Aagaard*, 1981].

3. Material and Methods

[6] The study is based on the lower 247 cm of the 883 cm long piston core MSM05/5-712-2 (78° 54′N, 06° 46′E). The core was recovered from 1487 m water depth from the western Svalbard margin in 2007 during a cruise with R/V "*Maria S. Merian*" (Figure 1a). The core was opened shortly after coring, and the lithology was described.

[7] The core section from 636 to 680 cm was subsampled in 1 cm thick slices for every 4 to 5 cm, and the remaining

Table 1. AMS^{14}C and Calibrated Dates Used in Age-Depth Model in Core MSM5/5-712-2

Lab No.	Depth (cm)	AMS ^{14}C yr BP	Reservoir-Corrected ^{14}C (−440 years *Mangerud and Gulliksen* [1975])	Calibrated Ages (BP ± 1σ)	δ^{13}C
Poz-30727	687–688	14,650 ± 75	14,210	16,660 ± 150	0.2
Poz-38427	716–716.5	17,200 ± 120	16,760	19,910 ± 160	0.1
Poz-30728	762–762.5	19,300 ± 140	18,860	22,440 ± 140	0.8
Poz-38428	780.5–781	20,390 ± 150[b]	19,950[b]	23,840 ± 190[b]	−2.5
—	800	20,150 ± 130[a]	19,710	23,550 ± 185	—
—	842	20,580 ± 150[a]	20,140	24,050 ± 150	—
Poz-30729	882.5–883	24,480 ± 190	24,040	28,780 ± 250	−1

[a]Chronological tie point from *Jessen et al*. [2010].
[b]Date not used in age model.

part from 680 to 883 cm was subsampled at different intervals at every 0.5, 1, or 2 cm. Wet bulk density was determined every 10–20 cm. The samples were freeze-dried and sieved through 1 mm, 100 µm, and 63 µm mesh sizes following the preparation methods described by *Feyling-Hanssen et al*. [1971] and *Knudsen* [1998]. Mineral grains >1 mm were counted and identified as ice-rafted debris (IRD). Planktic foraminifera were counted in the 100 µm–1 mm size fraction. At least 300 planktic foraminiferal specimens were picked from each sample and identified to species level. The total concentration (number of foraminifera specimens per gram dry weight sediment) and the relative abundances (%) of individual species of planktic foraminifera were calculated. Planktic foraminiferal species such as *Turborotalita quinqueloba*, *Neogloboquadrina incompta*, *Globigerinita glutinata*, and *Globigerina bulloide*s are subpolar species [*Bé and Tolderlund*, 1971; *Johannessen et al*., 1994; *Carstens et al*., 1997; *Simstich et al*., 2003], while *N. pachyderma* is a polar species [*Bé and Tolderlund*, 1971; *Johannessen et al*., 1994]. Following *Darling et al*. [2006], we refer *N. pachyderma* to sinistral forms and *N. incompta* to dextrally coiled forms. The method described by *Ehrmann and Thiede* [1985] was used to calculate the fluxes of planktic foraminiferal specimens (number of specimens)/(cm^2 × kyr) and IRD (grains)/(cm^2 × kyr). Dry bulk density was calculated based on water content and wet bulk density and corrected for the density of sea water.

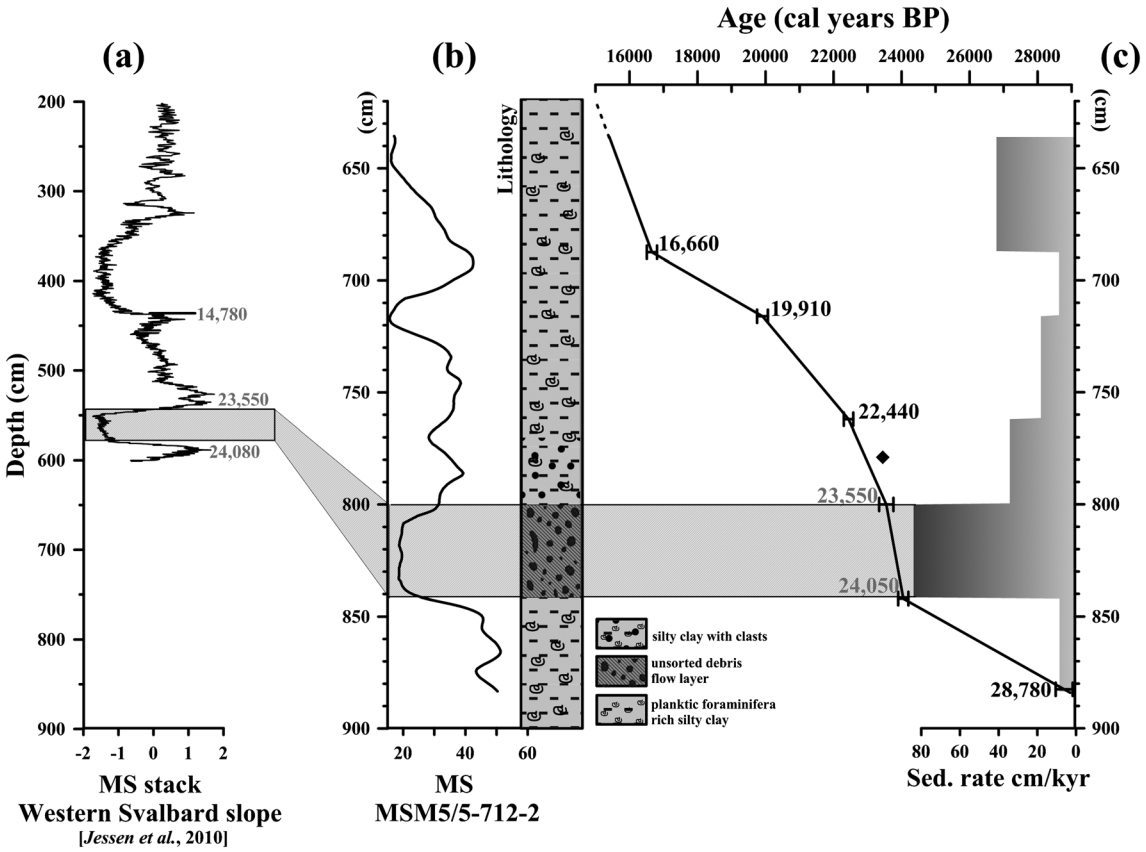

Figure 2. Correlation between (a) stacked magnetic susceptibility from the western Svalbard slope [*Jessen et al*., 2010] and (b) magnetic susceptibility and lithology records in the investigated interval in core MSM5/5-712-2. (c) Age model and average sedimentation rates in core MSM5/5-712-2. Ages in gray are from *Jessen et al*. [2010], and ages in black are from the present study. Hatched bar indicates position in the cores of the mass transport deposits.

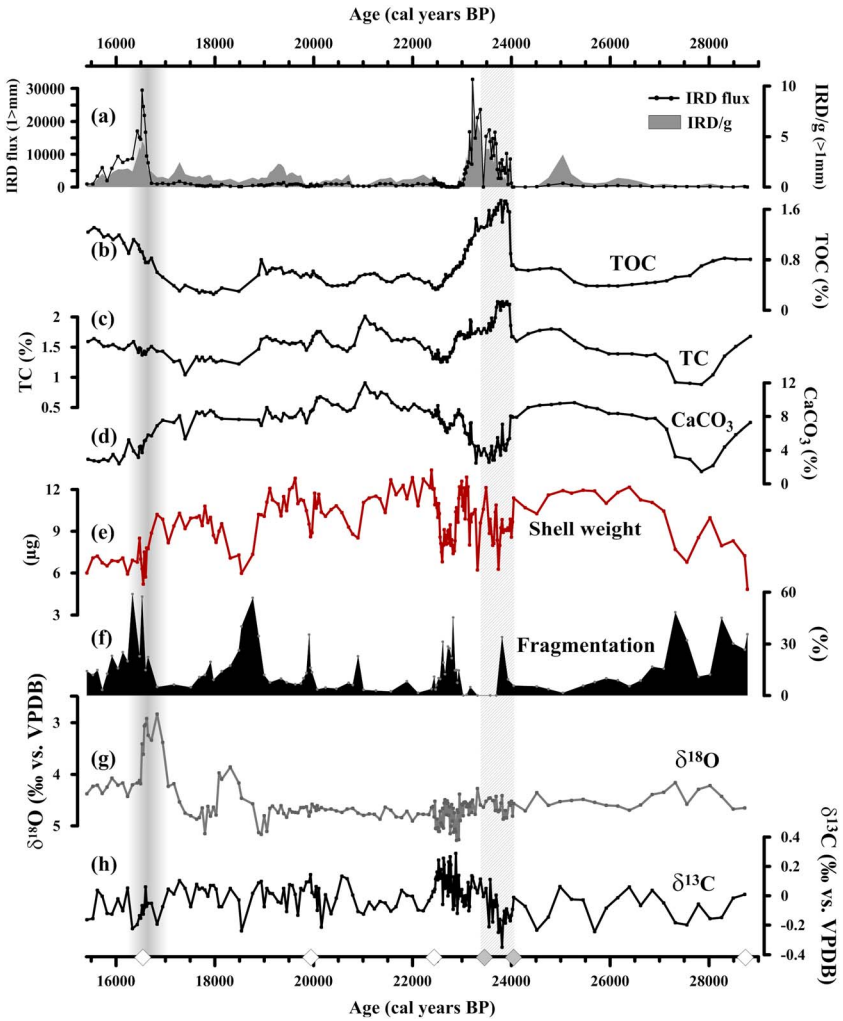

Figure 3. IRD, stable isotopes, and foraminiferal records plotted versus age in core MSM5/5-712-2. (a) concentration and flux of IRD, (b) %TOC, (c) %TC, (d) %$CaCO_3$, (e) mean shell weight of *N. pachyderma*, (f) %fragmentation, (g) $\delta^{18}O$, and (h) $\delta^{13}C$. Hatched and gray bars indicate mass transported deposit (part of Heinrich event H2; see *Jessen et al.* [2010]) and Heinrich event H1, respectively. White diamonds show the positions of radiocarbon dates. The gray diamonds show the tie points from *Jessen et al.* [2010].

[8] Shell weight as a measurement for preservation of calcium carbonate was quantified [*Lohmann*, 1995; *Barker and Elderfield*, 2002; *Barker et al.*, 2004; *de Villiers*, 2004; *Zamelczyk et al.*, 2012, 2013]. Shells of the planktic foraminiferal species *Neogloboquadrina pachyderma* were weighed using a Sartorius microbalance (model M2P, 0.1 µg sensitivity). Medium-sized shells were handpicked from a narrow size range of 150–212 µm. Mean shell weights were calculated by dividing the weighed mass of 20–30 individuals by the total number of foraminiferal shells. Due to low abundances of planktic foraminifera 13 weighed samples contained less than 10 individuals. Measurements were repeated 3 times. Shells with sediment fill or showing signs of mechanical corrosion at the outer shell surface or having secondary calcite crusts were avoided. We minimized problems of different ontogenetic stages during the life cycle of *N. pachyderma* by weighing square-shaped forms of a specific morphotype with four chambers [*Darling et al.*, 2006]. In addition, a fragmentation index was established following *Berger et al.* [1982]. The number of planktic shell fragments was counted, and the number of fragments per gram dry sediment was calculated. Percent fragmentation was calculated relative to the total numbers of planktic foraminifera and the total number of fragments in a sample.

[9] Total carbon (TC) and total organic carbon (TOC) were measured in bulk samples using a Leco CS-200 induction furnace instrument. The weight percentage (wt %) of TC and TOC was calculated in intervals of 0.5–5 cm. The $CaCO_3$ content (wt %) was calculated using the following equation: $CaCO_3 = (TC\text{-}TOC) \times 8.33$ [*Espitalié et al.*, 1977].

[10] Stable isotopes were measured on the previously weighed specimens of *N. pachyderma* (see above) at the Leibniz Laboratory for Radiometric Dating and Stable Isotope Research in Kiel, Germany, using an automated Carbo-Kiel device connected to a Finnigan MAT 253 and MAT 252 mass spectrometers. Results refer to the Vienna Pee Dee Belemnite (VPDB) standard. The external analytical reproducibility was <0.06‰ and <0.03‰ for $\delta^{18}O$ and $\delta^{13}C$, respectively. Measurements were carried out at 3–5 cm intervals from 636 to 678 cm and at 0.5–2 cm intervals from 678 cm down core.

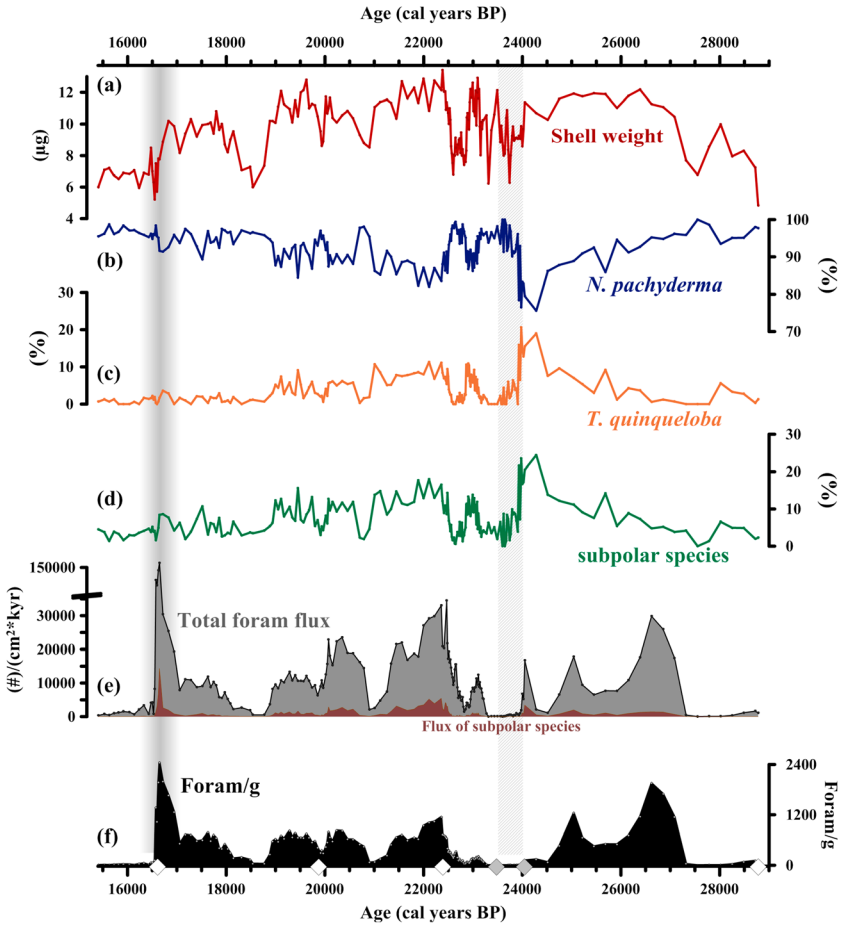

Figure 4. (a) Mean shell weight record and relative abundances of most frequent species (b) *N. pachyderma* and (c) *T. quinqueloba*, (d) % of subpolar species, (e) total flux and flux of subpolar species, and (f) concentration of planktic foraminifera in core MSM5/5-712-2. For legend, see Figure 3.

[11] Five accelerator mass spectrometry (AMS) ^{14}C ages performed on *N. pachyderma* were measured at Poznań Radiocarbon Laboratory (Table 1). The dates were corrected using a reservoir effect of 440 years [*Mangerud and Gulliksen*, 1975] and calibrated to calendar years before present using the Fairbanks 0701 data set (Table 1 and Figure 2) [*Fairbanks et al*., 2005].

[12] SiZer (significance of zero crossings of the derivative) analyses described by *Chaudhuri and Marron* [1999] were used to pinpoint statistically significant features in the variations of $CaCO_3$ content, mean shell weight, and abundance of subpolar species. The significance is defined based on whether the curve has a slope different from zero in a normal test statistic used by SiZer. If the test statistic is greater than a specified percentile in the standard distribution, the slope is considered as statistically significant. SiZer fits a local linear kernel estimator at a specific location. This means that a straight line is fitted using observations in a neighborhood of the point. The size of the neighborhood has the interpretation of a scale or a level of resolution for which the data are analyzed. The analysis use several neighborhood sizes; therefore, the data sets can be studied at a large number of different scales. A smoothing parameter entitled H represents the size of the neighborhood, meaning that a large H relates to a large neighborhood. As the true underlying curves at particular levels of resolution are identified and insignificant natural variability is removed, the measure of the true variation in the data sets is observed. The SiZer plot represents a graphical demonstration of statistically significant decreases or increases detected in the family plot.

4. Results

4.1. Lithology and Age Model

[13] The investigated interval comprises three different lithological units (Figure 2b). The lowermost unit from 883 to 842 cm is composed of hemipelagic light gray and homogenous silty clay rich in planktic foraminifera. The next unit from 842 to 800 cm consists of dark gray, coarse, unsorted glacigenic sediments with low content of foraminifera. The magnetic susceptibility values are low, and the sediment is interpreted as a debris flow deposit (see below). From 800 to 780.5 cm the sediments change gradually to hemipelagic light gray, foraminifera-rich, and homogenous silty clays that continue to the top of the studied section (Figure 2b). These characteristic sediments together with the pattern of magnetic susceptibility and the ^{14}C dates in the MSM5/5-712-2 core enable a close correlation to the stacked record of magnetic susceptibility published by *Jessen et al.* [2010] (Figures 2a and 2b). The stacked record is based on 11 cores from the western Svalbard slope. The coarse sediment layer characterized as a debris flow deposit has been dated from

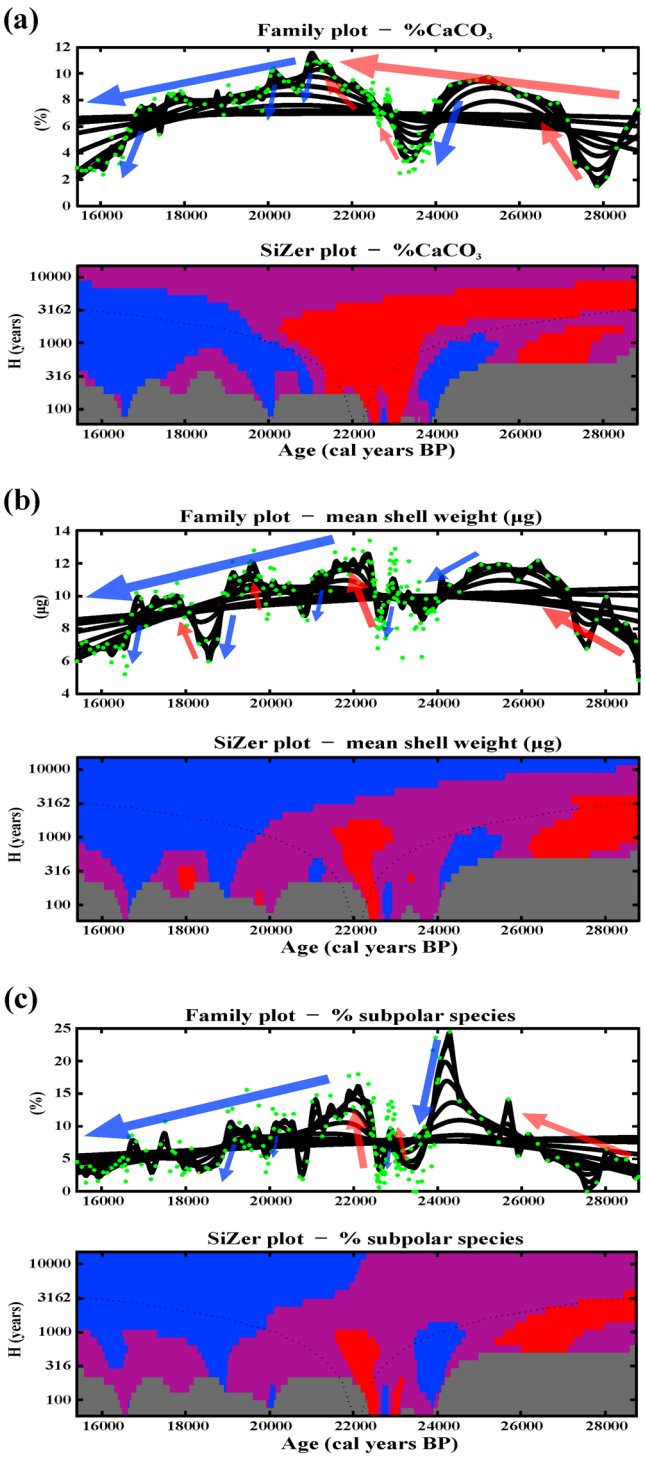

Figure 5. SiZer analysis of (a) $\%CaCO_3$, (b) mean shell weight of *N. pachyderma*, and (c) percent of subpolar species in core MSM5/5-712-2. Figures 5a–5c (top) show a family of smooths (H-values). The dots show original data points, and the black lines show the smoothing of these data from maximum to minimum values. Figures 5a–5c (bottom) show SiZer maps. A statistically significant increase is shaded in red and a decrease in blue. No change is indicated by purple and too few observations in grey. Red and blue arrows in the family panels mark significant increases and decreases in the original data set identified through SiZer analysis, respectively.

24.08 ± 0.15 to 23.55 ± 0.185 cal kyr [*Jessen et al.*, 2010]. These dates are used as chronological tie points dating the bottom and the top of the deposit at 842 and 800 cm depth, respectively (Figure 2). The age at 780.5–781.0 cm core depth shows an age of 23.84 ± 0.19 and is close to the age of the debris flow (23.55 ± 0.185 cal kyr) defined by *Jessen et al.* [2010]. However, the dated material at 780.5–781.0 cm originates from a narrow (0.5 cm) depth range where the admixture of old material is very likely. In addition, this date has a rather low-$\delta^{13}C$ value, which may have increased the error of the ^{14}C age in the sample (Table 1). Therefore, we used the two tie points of *Jessen et al.* [2010] for age of the debris flow deposit. The remaining radiocarbon dates and these two tie points are used to construct an age model based on linear interpolation between dating points (Table 1 and Figure 2c). The age model shows that the investigated sediment interval spans the time period 28.8–15.4 cal kyr comprising MIS 2 [*Martinson et al.*, 1987] and including the Last Glacial Maximum 23.0–19.0 kyr [*Yokoyama et al.*, 2000; *Mix et al.*, 2001]. The mean sedimentation rate is 18 cm/kyr. The sedimentation rates vary from 9 to 41 cm/kyr and reach up to 84 cm/kyr for the mass transported deposit (Figure 2c). The stratigraphic resolution is 54 years per 1 cm sample. In the following all ages will be reported in calibrated years unless otherwise stated.

4.2. IRD, Geochemistry, Shell Weight, Fragmentation and Stable Isotopes

[14] The flux and concentration of IRD >1 mm is generally low except for two intervals of high values at 24.1–23.0 and 16.6–15.6 kyr (Figure 3a). The events correlate in time with North Atlantic Heinrich events H2 (~24.0 kyr) and H1 (~17.0 kyr) [*Heinrich*, 1988] and are defined by low concentration of planktic foraminifera, dominance of *N. pachyderma*, high concentration of IRD, and low stable isotope values (Figures 3a, 3g, 4b, and 4f) [e.g., *Bond et al.*, 1993].

[15] The %TOC is low and stable from 28.8 to 16.8 kyr, except in the interval 24.1–~23 kyr, which is characterized by very high values (Figure 3b). From ~16.6 to 15.4 kyr the %TOC gradually increases. The %TC and $\%CaCO_3$ show a similar pattern except for intervals at 24.0–23.0 kyr and from ~17.2 to15.4 kyr (Figures 3c and 3d).

[16] The mean shell weight of *N. pachyderma* is generally very high (see discussion below) with intervals of generally reduced mean shell weight at ~28.8, 27.8–27.4, 24.1–22.5, 21.0–20.5, 18.8–18.3 and from 16.6 to15.4 kyr (Figure 3e). The fragmentation shows an opposite pattern to the mean shell weight record (Figure 3f).

[17] The $\delta^{18}O$ values are generally high except for two events of low values at 18.8–18.0 and 17.0–16.5 kyr (Figure 3g). The $\delta^{18}O$ values vary around an average of 4.7‰ from 28.8 to 18.8 kyr and around an average of 4.2‰ after 16.6 kyr. The $\delta^{13}C$ values vary between 0.23 and 0.23‰ with an average value of 0.06‰ (Figure 3h).

4.3. Planktic Foraminifera Assemblages and Fluxes

[18] The two dominant planktic foraminiferal species, *N. pachyderma* and *T. quinqueloba*, constitute 91–100% of the assemblages (Figures 4b and 4c). The relative abundance of *T. quinqueloba* shows generally the opposite distribution pattern of *N. pachyderma*. Other identified species, *N. incompta*, *G. glutinata*, and *G. bulloides*, are of low relative abundance. Generally, increases in the subploar species follow the increases

in mean shell weight (Figures 4a and 4d) with a correlation coefficient of 0.63.

[19] The total flux and the concentration of planktic specimens are overall high except for intervals at 28.8–27.4, 24.1–23.5, 21.2–20.8, and 18.8–18.3 and from 16.6–15.4 kyr (Figures 4e and 4f). These periods correlate with intervals of low shell weight of *N. pachyderma* (Figure 4a).

4.4. Sizer Analysis

[20] Based on the lithological features of the sediment, the rather high sedimentation rates and the many abrupt changes in our proxies (Figures 2–4), we assume that our observations are independent. The SiZer analysis define the following significant changes in the data sets: At the multimillennial bandwidth $\%CaCO_3$ increases from 28.8 to 20.1 kyr BP (Figure 5a). At the millennial and millennial to multicentennial bandwidth significant increases in $\%CaCO_3$ are observed at 28.6–26.0 and 23.8–~21.0 kyr. From ~21.0 to 15.4 kyr a decrease on the same time scale occurs. Several short-lasting decreases in $\%CaCO_3$ characterize the underlying multicentennial to decadal time scale.

[21] The mean shell weight shows decreasing trend on a 10 kyr scale (Figure 5b). However, marked increases occur from 28.8 to ~26.0 and from ~23.0 to 21.5 kyr on a lower H (years) scale. In addition, significant short-lasting increases are depicted at ~23.3, 22.3, 19.8, and ~18.0 kyr at multidecadal to multicentennial scale. A reduction in foraminiferal shell weight is found for the interval 20.0–15.4 kyr (Figure 5b).

[22] The sum of percent of *T. quinqueloba*, *N. incompta*, *G. glutinata*, and *G. bulloide*s shows a similar development as the mean shell weight at all nearly investigated time scales. At the multidecadal time scale two of the short-lasting increases at ~19.8 and ~18.0 kyr are not detected (Figure 5c).

5. Discussion

5.1. Planktic Foraminifera, Calcium Carbonate Preservation, and Dissolution Mechanisms on the Western Svalbard Slope

[23] In paleoceanographic interpretations in the polar North Atlantic a low concentration and flux of planktic foraminifera, the dominance of the polar species *N. pachyderma*, and low percentages of the subpolar species (*T. quinqueloba*, *N. incompta*, *G. glutinata*, and *G. bulloides*) indicate cold conditions at the sea surface. Oppositely, high flux of planktic foraminifera and higher relative abundance of subpolar species indicate warming of the surface water and probably a stronger advection of Atlantic water (Figure 4). In the Fram Strait, *T. quinqueloba* is abundant in the productive Arctic surface water and near the Arctic front between Arctic and Atlantic water masses [*Bé and Tolderlund*, 1971; *Johannessen et al.*, 1994; *Carstens et al.*, 1997; *Simstich et al.*, 2003]. Hence, high abundance of this species is considered to represent an enhanced influence of Atlantic water and proximity of the oceanic front. In addition, high numbers of planktic foraminifera are related to high primary productivity [*Carstens et al.*, 1997]. Intervals with high %TOC and low $\%CaCO_3$ imply the presence of seasonal sea ice and Arctic surface water [*Zamelczyk et al.*, 2012, 2013, and references herein] and the high concentration and flux of IRD indicate the presence of icebergs (Figure 3).

[24] Overall, we observe a covariance of the dissolution proxies (mean shell weight, $\%CaCO_3$ and %fragmentation) with the distribution of the foraminiferal species and the concentration and flux of planktic specimens (Figures 3–5) (see section 4.3.). This implies that many of the changes can be a result of dissolution effects superimposed on the changes in the distribution of water masses and surface productivity. Below we explore the variations in paleoceanography and preservation of planktic specimens on the West Spitsbergen continental margin.

[25] The MSM5/5-712-2 record shows overall high planktic foraminifera shell weight between 28.8 and 15.4 kyr (Figures 3e and 4a). Decreases in shell weight correlate with increases in %fragmentation and low $\%CaCO_3$ (with a correlation coefficient of 0.6 and 0.48, respectively) during the entire investigated time period (Figures 3d–3f). This signifies that dissolution occurred repeatedly on a multicentennial time scale during MIS 2 (28.8–27.2, 24.1–23.2, and 16.6–15.4 kyr). During the LGM to the early deglaciation several short-lasting episodes of poorer preservation occur (22.8–22.5, 21.0–20.5, 20.0–19.8, and 18.8–18.3 kyr) (Figures 3–5). The three longer-lasting events also correlate with high %TOC (Figure 3b). The SiZer analyses pointed out that most of the events are statistically significant (Figure 5).

[26] The subpolar species (*T. quinqueloba*, *N. incompta*, *G. glutinata*, and *G. bulloides*) are all more prone to dissolution than *N. pachyderma* [*Berger*, 1970]. Small and thin-walled specimens of *T. quinqueloba* have been shown to be especially vulnerable to dissolution [*Berger*, 1970]. Studies of Holocene and glacial records from the Fram Strait reveal that this species generally covaries in relative abundance with the degree of dissolution in the sediment [*Bauch et al.*, 2001; *Rasmussen et al.*, 2007; *Zamelczyk et al.*, 2012, 2013]. Therefore, it is probable that many of the changes in the distribution patterns of the planktic foraminifera are partly a result of changes in preservation.

[27] In the Arctic Ocean, the saturation horizon of calcite is located at ~4000 m [*Jutterström and Anderson*, 2005]. During glacial time, the calcium carbonate saturation depth is believed to be similar to the modern depth [*Catubig et al.*, 1998]. The core MSM5/5-712-2 is positioned well above this level implying that factors other than undersaturation of calcite must have caused the dissolution of the calcium carbonate. Therefore, we argue below that the periods with poorer preservation of calcium carbonate can be attributed to periods of spread of Arctic surface water masses and associated increased primary soft-tissue productivity within the marginal ice zone (MIZ). Periods with good preservation can thus probably be linked to the influence of Atlantic water masses with higher productivity of calcareous organisms and decreased sea ice cover.

[28] In the modern northern North Atlantic, preservation of calcium carbonate reflects the circulation of the surface water and the intensity and quality of the primary productivity at the surface. Well-preserved carbonate shells are found along the inflow of warm Atlantic surface water, while poor-preserved shells are observed under the influence of cold water masses [*Henrich*, 1998; *Huber et al.*, 2000]. In core MSM5/5-712-2, changes in species composition of planktic foraminifera and calcium carbonate preservation indicate that changing intensity of the Atlantic water inflow was the common factor controlling changes in carbonate preservation during the late glacial and early deglaciation in the Fram Strait

(Figures 3d–3f and 4) [see also *Zamelczyk et al*., 2012, 2013]. Studies based on the geochemistry of planktic foraminiferal shells show that the rate of calcification and the shell weight depends on the concentration of CO_3^{2-} in the surface waters [*Bijma et al*., 1999; *Barker and Elderfield*, 2002]. Arctic waters are characterized by lower concentration of CO_3^{2-} than Atlantic waters [*Chierici and Fransson*, 2009; *Azetsu-Scott et al*., 2010], and the decrease in the mean shell weight of the foraminifera may reflect the influence of Arctic water masses. However, interpretation of the CO_3^{2-} effect on calcifying planktic foraminifera is not straightforward, because the carbonate ion content may covary with seasonal shifts in surface water temperature [*Gonzalez-Mora et al*., 2008], nutrient availability [*de Villiers*, 2004], and/or salinity [*Hönisch*, 2002]. In addition, the high organic productivity (primarily soft-tissue organisms) may lead to undersaturation of $CaCO_3$ in the sediment [*Emerson and Bender*, 1981; *Scott et al*., 2008]. In the Fram Strait, Arctic water masses control the position of the Arctic front and the sea ice margin. Seasonal primary production within marginal ice zones (MIZs) generated along a stationary sea ice margin can be markedly higher than under ice free conditions [*Smith and Sakshaug*, 1990; *Johannessen et al*., 1994; *Carstens et al*., 1997]. Enhanced fluxes of organic particles and the acidity produced by oxidation of organic material at and within the sediments are an important mechanism for carbonate dissolution [*Emerson and Bender*, 1981]. Calcite dissolution within carbonate-rich sediments below the Atlantic water flow is unlikely due to the high buffering potential [e.g. *Huber et al*., 2000. However, pronounced increase in rain ratio of organic and inorganic ($CaCO_3$) carbons may cause enhanced respirative release of CO_2, to an extent where it cannot be compensated by buffering. This can lead to calcium carbonate dissolution even in carbonate-rich surface sediments [e.g., *Huber et al*., 2000].

[29] In core MSM5/5-712-2, the apparent anticorrelation between the relative abundance and shell weight of *N. pachyderma* and distribution patterns of subpolar species indicate that whenever the high productive Arctic waters invaded the study site, the preservation of calcium carbonate deteriorated (Figures 4a and 4d). The selective removal of subpolar species through dissolution potentially exaggerates the cooling signal observed in paleorecord. The high fragmentation of shells, low shell weight, and low $CaCO_3$ content indicate that the spread of Arctic water masses associated with changes in the carbonate rain ratio of organic and inorganic ($CaCO_3$) carbon fluxes most likely promoted dissolution of calcium carbonate.

5.2. Comparison to Other Areas and Implications for Preservation

[30] We compare our dissolution proxies and absolute and relative abundances of planktic foraminifera with other published records of foraminiferal distribution patterns from the Nordic Seas. All are located in the pathway of the inflow of Atlantic water.

[31] In the northern North Atlantic, surface conditions of the MIS 2, including the LGM and the early deglaciation, were characterized by cold but seasonally open waters [e.g., *Peck et al*., 2006, 2008; *Knutz et al*., 2007; *Rasmussen and Thomsen*, 2008; *Scourse et al*., 2009]. In the Fram Strait, the Atlantic water inflow was variable but sufficiently strong to allow for enhanced production of planktic foraminifera [*Hebbeln et al*., 1994; *Dokken and Hald*, 1996; *Knies et al*., 1999; *Hald et al*., 2001; *Nørgaard-Pedersen et al*., 2003; *Rasmussen et al*., 2007]. The results from the core MSM5/5-712-2 show that the Atlantic surface water was generally present and favored the preservation of planktic foraminifera for most of the glacial period (Figures 3 and 4).

[32] Between 24.1 and 22.5 kyr in core MSM5/5-712-2, the carbonate preservation is very poor, the number of planktic foraminifera very low, and the fauna is completely dominated by *N. pachyderma* (Figure 4b). At the Yermak Plateau, absence of planktic foraminifera and an enhanced sea ice cover occurred at the same time [*Nørgaard-Pedersen et al*., 2003; *Müller et al*., 2009]. This suggests spread of very cold Arctic surface waters with drifting icebergs and dense sea ice cover. Similar sea surface conditions have been described in southerly located cores, LINK17 and ENAM93-21 from the Faeroe-Shetland Channel [*Rasmussen et al*., 1997; *Rasmussen and Thomsen*, 2008] and DAPC2 and several records from off the British Islands [*Knutz et al*., 2007; *Scourse et al*., 2009]. They are also in agreement with low temperatures reconstructed from Mg/Ca ratios in planktic foraminifera from south of the British Islands [*Peck et al*., 2008]. The seasonal sea ice in the North Atlantic is suggested to reach as far south as 40°N during this time [*Heinrich*, 1988; *Bond et al*., 1992, 1999; *Mix et al*., 2001; *Pflaumann et al*., 2003]. Between 55°N and 40°N, these conditions are attributed to the North Atlantic Heinrich event H2.

[33] During the early deglaciation, from ~19.0 to 15.4 kyr, the Atlantic water inflow at the MSM5/5-712-2 progressively weakened and the surface waters continued to cool (Figure 4). Similar oceanic development is observed in the North Atlantic Ocean area [e.g., *McManus et al*., 2004; *Hall et al*., 2006; *Stanford et al*., 2011]. It is believed that from ~19.0 kyr, the fresh water were progressively supplied to the surface of the North Atlantic Ocean and led to a reduction of the oceanic poleward heat transport by a gradual slowdown of the Atlantic meridional overturning circulation [e.g., *McManus et al*., 2004; *Hall et al*., 2006; *Stanford et al*., 2011]. The interval shows a general deterioration of preservation of calcium carbonate with poor preservation at ~19.0–18.0 kyr and ~16.6–15.4 kyr (Figures 3d–3f). From ~18.0 to 16.6 kyr, improved preservation and rising concentrations of planktic foraminifera and dominance of polar *N. pachyderma* indicate presence of cold water masses in the eastern Fram Strait (Figures 3d–3f, 4b, and 4f). In the North Atlantic, the change to extreme cold conditions correlates with the collapse of the thermohaline circulation at ~17.5 kyr [*McManus et al*., 2004; *Hall et al*., 2006; *Stanford et al*., 2011] and is attributed to H1 [*Heinrich*, 1988; *Bond et al*., 1992, 1993, 1999]. The preservation of carbonates increases in the beginning of the H1, whereas the preservation is very poor after 16.6 kyr (Figures 3 and 4). This is in agreement with studies on dissolution of planktic foraminiferal shells from the North Atlantic (cores British Ocean Flux Study 17 K and NEAP 8 K) [*Barker et al*., 2004]. It was proposed that the stratification of the water masses during the early stages of H1 and the reinforced ventilation of the Atlantic waters toward the end of H1 and the start of the Bølling interstadial caused the sudden shift in preservation of carbonates in the northern North Atlantic [*Barker et al*., 2004].

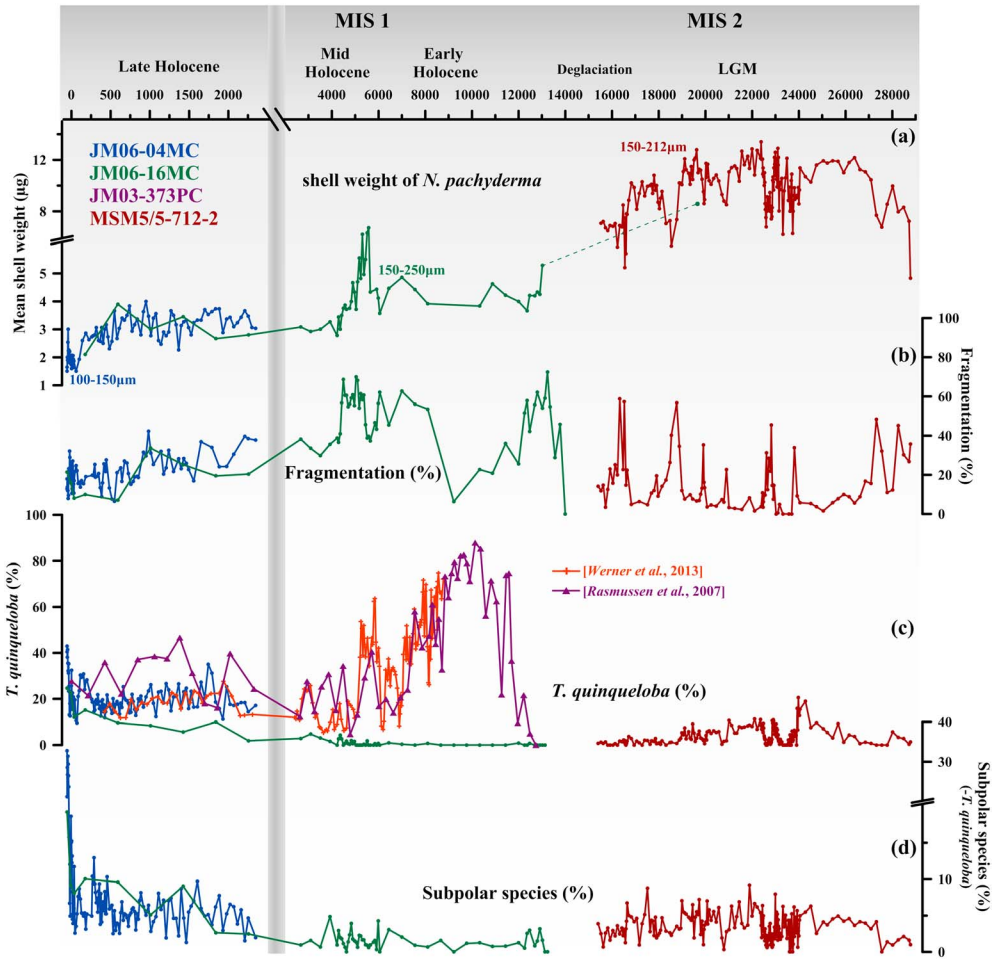

Figure 6. Comparison of (a) mean shell weight of *N. pachyderma*, (b) %fragmentation, (c) %*T. quinqueloba*, and (d) % of subpolar species (*N. incompta*, *G. glutinata*, and *G. bulloides*) from the Fram Strait covering the last ~29 kyr. Graphs in red and light red color represent data from core MSM5/5-712-2 (this study and *Werner et al.* [2013], respectively). Graph in purple color shows data from core JM03-373PC [*Rasmussen et al.*, 2007]. Graphs in green and blue show data from cores JM06-16MC and JM06-04MC, respectively [*Zamelczyk et al.*, 2012, 2013].

6. Comparison of MIS 2 and Holocene Preservation Records in the Fram Strait

[34] In order to obtain a broader perspective of the preservation history from the Fram Strait, we compare available records of mean shell weight, %fragmentation and distribution patterns of subpolar species (Figure 6). Core JM06-04MC is from the same position as the MSM5/5-712-2 core and spans the last 2400 years. The cores are from the eastern Fram Strait influenced by warm Atlantic water masses [*Zamelczyk et al.*, 2013]. Core JM06-16MC is from the central Fram Strait from 2546 m water depth and comprises the last 20 kyr (Figures 1a and 6) [*Zamelczyk et al.*, 2012]. The core site is dominated by Arctic water masses with reduced $CaCO_3$ saturation and seasonal high primary production. This record generally shows poor preservation of planktic shells and low relative abundance of *T. quinqueloba* and other subpolar planktic species (Figures 6c and 6d).

[35] The compiled shell weight record shows a clear decreasing trend throughout the last ~29 kyr. Highest shell weights, with a maximum of 13.4 µg, occur during the LGM (22.5–19.0 kyr). The shell weights decrease toward the present day (2006 AD) [see *Zamelczyk et al.*, 2012, 2013] to a minimum of 1.5 µg (Figure 6a). During MIS 2 the change in shell weights correlates closely with increases in %fragmentation, while the correlation is less direct in the Holocene part (Figures 6a and 6b). The percentages of *T. quinqueloba* and subpolar species also show a clear anticorrelation to the fragmentation record from ~29.0 to ~19.0 kyr and again from ~14 kyr and in the early to mid-Holocene (Figures 6c and 6d) [see also *Rasmussen et al.*, 2007; *Zamelczyk et al.*, 2012]. The trend is interrupted in the late Holocene (the last ~2.5 kyr), when the relative abundance of *T. quinqueloba* and subpolar species increase, which would indicate a warming (Figures 6c and 6d). However, together with the low and decreasing shell weight the changes in the composition of the planktic foraminiferal faunas are more likely due to still ongoing diagenetic processes in the sediments (see discussion in *Zamelczyk et al.* [2012, 2013]).

[36] The combined record of the preservation proxies and the distribution patterns of foraminiferal species imply that the expansion of Arctic water masses associated with changes

in the carbonate rain ratio of organic and inorganic carbon fluxes in the Fram Strait most likely played a dominant role in preservation of calcium carbonate over the entire last ~29 kyr. From the culmination of the LGM, relatively fresh Arctic water masses with low $CaCO_3$-saturation state spread southeastward. The progressive influence of Arctic waters during the deglaciation caused extensive dissolution of calcium carbonate (Figure 6). Preservation deteriorated again from the late early Holocene to today.

[37] We note that events of lower shell weight and higher fragmentation and hence poorer preservation during MIS 2 rarely exceed the values found in the Holocene (Figures 6a and 6b). The observed patterns of preservation from a maximum in MIS 2 to a minimum during the Holocene cannot only be related to changes in the distribution of surface water masses but may also be linked to the impact of changes in atmospheric concentration of carbon dioxide (CO_2) on the surface water chemistry [e.g., *Bijma et al*., 2002; *Bates and Mathis*, 2009]. Changes in atmospheric CO_2 coincide with higher pH and a higher carbonate ion (CO_3^{2-}) concentration during glacials and lower concentration during interglacials [*Sanyal et al*., 1995; *Hönisch and Hemming*, 2005; *Foster*, 2008]. Therefore, we speculate that the low concentration of atmospheric CO_2 during MIS 2 [e.g., *Broecker and Peng*, 1987; *Sigman and Boyle*, 2000; *Sigman et al*., 2010] contributed to the good preservation of $CaCO_3$, and vice versa, the increased CO_2 concentrations during the Holocene enhanced the dissolution of $CaCO_3$. The lower pH and a lower carbonate ion concentration during the deglaciation and the Holocene probably decreased the calcification of the planktic foraminifera. The reduced calcification resulted in thinner shells making them even more vulnerable to corrosive conditions.

7. Conclusions

[38] In general, the results confirm previous reconstructions of oceanography of the late glacial and early deglaciation in the Fram Strait. Ice-free conditions and high planktic foraminiferal productivity predominated during the glacial summers. High abundances of subpolar species were found during periods of influence of Atlantic water and the preservation of calcium carbonate was good to excellent. Simultaneous decreases in preservation, subpolar species, and planktic foraminifera abundances are attributed to periods when Arctic surface waters with low $CaCO_3$-saturation and/or the highly productive marginal ice zone approached the study site. During these periods, the planktic foraminiferal fauna was completely dominated by the polar species *N. pachyderma*, which is also less susceptible to dissolution. These intervals of enhanced dissolution occurred on the western Svalbard slope at 28.8–27.2, 24.1–23.2, and 16.6–15.4 kyr and were characterized by low mean shell weight and low percentages of dissolution-prone subpolar specimens, high shell fragmentation, and reduced content of $CaCO_3$. Short-lasting events of poorer preservation also occurred during the LGM.

[39] The periods of poor preservation of calcium carbonate imply selective removal of species that are more susceptible to dissolution and therefore may have reduced the reliability of paleoceanographic reconstructions in the Fram Strait for the cold periods during the last ~29 kyr.

[40] **Acknowledgments.** The core was retrieved by the R/V "*Maria S. Merian*" during the MSM05/5b expedition led by Gereon Budeus, Alfred Wegener Institute for Polar and Marine Research, Germany. The study was a part of the International Polar Year project (IPY project no. 39) "Arctic Natural Climate and Environmental Changes and Human Adaptation: From Science to Public Awareness (SciencePub)," "Effects of ocean chemistry changes on planktic foraminifera in the Fram Strait: Ocean Acidification from natural to anthropogenic changes," and "Centre for Arctic Gas Hydrates, Environment and Climate (CAGE)," all funded by the Research Council of Norway and the University of Tromsø. Funding from Statoil is also acknowledged. We kindly thank Robert F. Spielhagen for availability of the sediment core and Steffen Aagaard Sørensen for helpful comments and discussions. This article greatly benefited from the constructive reviews by Christopher Charles, Andreas Mackensen, and an anonymous reviewer. Jan. P. Holm helped prepare the bathymetric map.

References

Azetsu-Scott, K., A. Clarke, K. Falkner, J. Hamilton, E. P. Jones, C. Lee, B. Petrie, S. Prinsenberg, M. Starr, and P. Yeats (2010), Calcium carbonate saturation states in the waters of the Canadian Arctic Archipelago and the Labrador Sea, *J. Geophys. Res.*, *115*, C11021, doi:10.1029/2009JC005917.

Barker, S., and H. Elderfield (2002), Foraminiferal calcification response to glacial-interglacial changes in atmospheric CO_2, *Science*, *297*, 833, doi:10.1126/science.1072815.

Barker, S., T. Kiefer, and H. Elderfield (2004), Temporal changes in North Atlantic circulation constrained by planktonic foraminiferal shell weights, *Paleoceanography*, *19*, PA3008, doi:10.1029/2004PA001004.

Bates, N. R., and J. T. Mathis (2009), The Arctic Ocean marine carbon cycle: Evaluation of air-sea CO_2 exchanges, ocean acidification impacts and potential feedbacks, *Biogeosciences*, *6*, 2433–2459.

Bauch, H. A., H. Erlenkeuser, R. F. Spielhagen, U. Struck, J. Matthiessen, J. Thiede, and J. Heinemeier (2001), A multiproxy reconstruction of the evolution of deep and surface waters in the subarctic Nordic seas over the last 30,000 yr, *Quat. Sci. Rev.*, *20*, 659–678, doi:10.1016/S0277-3791(00)00098-6.

Bé, A. W. H., and D. S. Tolderlund (1971), Distribution and ecology of living planktonic foraminifera in surface waters of the Atlantic and Indian Oceans, in *The Micropaleontology of the Oceans*, edited by B. M. Funnel and W. R. Riedel, pp. 105–144, Cambridge Univ. Press, Cambridge, UK.

Berger, W. H. (1970), Planktonic foraminifera: Selective solution and the lysocline, *Mar. Geol.*, *8*, 111–138.

Berger, W. H., M.-C. Bonneau, and F. L. Parker (1982), Foraminifera on the deep-sea floor: Lysocline and dissolution rate, *Oceanol. Acta*, *5*, 249–258.

Bijma, J., H. J. Spero, and D. W. Lea (1999), Reassessing foraminiferal stable isotope geochemistry: Impact of the oceanic carbonate system (experimental results), in *Use of Proxies in Paleoceanography: Examples From the South Atlantic*, edited by G. Fischer and G. Wefer, pp. 489–512, Springer-Verlag, Berlin, Heidelberg.

Bijma, J., B. Hönisch, and R. E. Zeebe (2002), Impact of the ocean carbonate chemistry on living foraminiferal shell weight: Comment on "Carbonate ion concentration in glacial-age deep waters of the Caribbean Sea" by Broecker, W. S., and E. Clark, *Geochem. Geophys. Geosyst.*, *3*(11), 1064, doi:10.1029/2002GC000388.

Bond, G. W., et al. (1992), Evidence for massive discharges of icebergs into the North Atlantic Ocean during the last glacial period, *Nature*, *360*, 245–249.

Bond, G., W. S. Broecker, S. J. Johnsen, J. McManus, L. Labeyrie, J. Jouzel, and G. Bonani (1993), Correlations between climate records from North Atlantic sediments and Greenland ice, *Nature*, *365*, 143–147.

Bond, G., W. Showers, M. Elliot, M. Evans, R. Lotti, I. Hajdas, G. Bonani, and S. Johnson (1999), The North Atlantic's 1–2 kyr climate rhythm: Relation to Heinrich events, Dansgaard/Oeschger cycles and the little ice age, in *Mechanisms of Global Climate Change at Millennial Time Scale*, edited by P. U. Clark, R. S. Webb, and L. D. Keigwin, pp. 35–58, American Geophysical Union, Washington, D. C.

Broecker, W. S., and T. H. Peng (1987), The role of $CaCO_3$ compensation in the glacial to interglacial CO_2 change, *Global Biogeochem. Cycles*, *1*, 15–29.

Carstens, J., D. Hebbeln, and G. Wefer (1997), Distribution of planktic foraminifera at the ice margin in the Arctic (Fram Strait), *Mar. Micropaleontol.*, *29*(3–4), 257–269.

Catubig, N. R., D. E. Archer, R. Francois, P. deMenocal, W. R. Howard, and E. F. Yu (1998), Global deep-sea burial rate of calcium carbonate during the last glacial maximum, *Paleoceanography*, *13*(3), 298–310.

Chaudhuri, P., and J. S. Marron (1999), SiZer for exploration of sturctures in curves, *J. Am. Stat. Assoc.*, *94*, 807–823.

Chierici, M., and A. Fransson (2009), Calcium carbonate saturation in the surface water of the Arctic Ocean: Undersaturation in freshwater influenced shelves, *Biogeosciences*, *6*, 2421–2432.

Darling, K. F., M. Kucera, D. Kroon, and C. M. Wade (2006), A resolution for the coiling direction paradox in *Neogloboquadrina pachyderma*, *Paleoceanography*, *21*, PA2011, doi:10.1029/2005PA001189.

de Vernal, A., A. Rosell-Melé, M. Kucera, C. Hillaire-Marcel, F. Eynaud, M. Weinelt, T. Dokken, and M. Kageyama (2006), Comparing proxies for the reconstruction of LGM sea-surface conditions in the northern North Atlantic, *Quat. Sci. Rev.*, *25*(21–22), 2820–2834, doi:10.1016/j.quascirev.2006.06.006.

de Villiers, S. (2004), Occupation of an ecological niche as the fundamental control on the shell weight of calcifying planktonic foraminifera, *Mar. Biol.*, *144*(1), 45–50.

Dokken, T. M., and M. Hald (1996), Rapid climatic shifts during isotope stages 2–4 in the Polar North Atlantic, *Geology*, *24*(7), 599–602.

Ehrmann, W. U., and J. Thiede (1985), History of Mesozoic and Cenozoic sediments fluxes to the North Atlantic Ocean, in *Contributions to Sedimentology, E. Schweizerbart'sche Verlagsbuchhandlung (Nägele u. Obermiller)*, vol. 15, edited by H. Füchtbauer, A. P. Lisitzyn, J. D. Milliman, and E. Seibold, pp. 1–109, Schweizerbart, Stuttgart.

Emerson, S., and M. Bender (1981), Carbon fluxes at the sediment-water interface of the deep-sea: Calcium carbonate preservation, *J. Mar. Res.*, *39*, 139–162.

Espitalié, J., J. L. Laporte, M. Madec, F. Marquis, P. Leplat, J. Paulet, and A. Boutefeu (1977), Méthode rapide de characterisation des roches-mere, de leur potential petrolier et de leur degre d'évolution, *Rev. Inst. Tranc. Petrol.*, *32*, 23–42.

Fairbanks, R. G., R. A. Mortlock, T.-C. Chiu, L. Cao, A. Kaplan, T. P. Guilderson, T. W. Fairbanks, A. L. Bloom, P. M. Grootes, and M. J. Nadeau (2005), Radiocarbon curve spanning 0 to 50,000 years BP based on paired $^{230}TH/^{234}U/^{238}U$ and ^{14}C dates on pristine corals, *Quat. Sci. Rev.*, *24*, 1781–1796.

Feyling-Hanssen, R. W., J. A. Jorgensen, K. L. Knudsen, and A. L. Anderson (1971), Late Quaternary foraminifera from Vendsyssel Denmark and Sandnes, Norway, *Bull. Geol. Soc. Den.*, *21*, 67–317.

Foster, G. L. (2008), Seawater pH, pCO_2 and $[CO_3^{2-}]$ variations in the Caribbean Sea over the last 130kyr: A boron isotope and B/Ca study of planktic foraminifera, *Earth Planet. Sci. Lett.*, *271*(1–2), 290–291, doi:10.1016/j.epsl.2008.10.001.

Gonzalez-Mora, B., F. J. Sierro, and J. A. Flores (2008), Controls of shell calcification in planktonic foraminifers, *Quat. Sci. Rev.*, *27*, 956–961, doi:10.1016/j.quascirev.2008.01.008.

Hald, M., T. Dokken, and G. Mikalsen (2001), Abrupt climate change during the last interglacial-glacial cycle in the polar North Atlantic, *Mar. Geol.*, *176*(1), 121–137.

Hall, I. R., S. B. Moran, R. Zahn, P. C. Knutz, C. C. Shen, and R. L. Edwards (2006), Accelerated drawdown of meridional overturning in the late-glacial Atlantic triggered by transient pre-H event freshwater perturbation, *Geophys. Res. Lett.*, *33*, L16616, doi:10.1029/2006GL026239.

Hebbeln, D., and G. Wefer (1997), Late Quaternary palaeoceanography in the Fram Strait, *Palaeoceanography*, *12*(1), 65–78.

Hebbeln, D., T. Dokken, E. S. Andersen, M. Hald, and A. Elverhøi (1994), Moisture supply for northern ice-sheet growth during the Last Glacial Maximum, *Nature*, *370*, 357–360.

Hebbeln, D., R. Henrich, and K. H. Bauman (1998), Paleoceanography of the last interglacial/glacial cycle in the Polar North Atlantic, *Quat. Sci. Rev.*, *17*(1–3), 125–153.

Heinrich, H. (1988), Origin and consequences of cyclic ice rafting in the Northeast Atlantic Ocean during the past 130,000 years, *Quat. Res.*, *29*(2), 142–152.

Hemleben, C., M. Spindler, and O. R. Anderson (1989), *Modern Planktonic Foraminifera*, pp. 363 , Springer-Verlag, New York.

Henrich, R. (1998), Dynamics of Atlantic water advection to the Norwegian-Greenland Sea time slice record of carbonate distribution in the last 300 ky, *Mar. Geol.*, *145*(1–2), 95–131.

Hönisch, B. (2002), Stable isotope and trace element composition of foraminiferal calcite—From incorporation to dissolution, *PhD thesis*, Bremen, hdl:10013/epic.18483.

Hönisch, B., and N. G. Hemming (2005), Surface ocean pH response to variations in pCO_2 through two full glacial cycles, *Earth Planet. Sci. Lett.*, *236*(1–2), 305–314, doi:10.1016/j.epsl.2005.04.027.

Hop, H., S. Falk-Petersen, H. Svendsen, S. Kwasniewski, V. Pavlov, O. Pavlova, and J. E. Søreide (2006), Physical and biological characteristics of the pelagic system across Fram Strait to Kongsfjorden, *Prog. Oceanogr.*, *71*, 182–231, doi:10.1016/j.pocean.2006.09.007.

Huber, R., H. Meggers, K. H. Baumann, and R. Henrich (2000), Recent and Pleistocene carbonate dissolution in sediments of the Norwegian-Greenland Sea, *Mar. Geol.*, *165*, 123–136.

Jessen, S. P., T. L. Rasmussen, T. Nielsen, and A. Solheim (2010), A new Late Weichselian and Holocene marine chronology for the western Svalbard slope 30,000-0 cal years BP, *Quat. Sci. Rev.*, *29*(9–10), 1301–1312, doi:10.1016/j.quascirev.2010.02.020.

Johannessen, T., E. Jansen, A. Flatøy, and A. C. Ravelo (1994), The relationship between surface water masses, oceanographic fronts and paleoclimatic proxies in surface sediments of the Greenland, Iceland, Norwegian Seas, *NATO ASI Series*, *117*, 61–86.

Jutterström, S., and L. G. Anderson (2005), The saturation of calcite and aragonite in the Arctic Ocean, *Mar. Chem.*, *94*(1–4), 101–110, doi:10.1016/j.marchem.2004.08.010.

Knies, J., and R. Stein (1998), New aspects of organic carbon deposition and paleoceanographic implications along the northern Barents Sea margin during the last 30,000 years, *Paleoceanography*, *13*(4), 384–394.

Knies, J., C. Vogt, and R. Stein (1999), Late Quaternary growth and decay of the Svalbard/Barents Sea ice-sheet and paleoceanographic evolution in the adjacent Arctic Ocean, *Geo Mar. Lett.*, *18*, 195–202.

Knudsen, K. L. (1998), Foraminiferer i Kvartær stratigrafi: Laboratorie og fremstillingsteknik samt udvalgte eksempler, *Geol. Tidsskr.*, *3*, 1–25.

Knutz, P. C., R. Zahn, and I. R. Hall (2007), Centennial-scale variability of the British Ice Sheet: Implications for climate forcing and Atlantic meridional overturning circulation during the last deglaciation, *Paleoceanography*, *22*, PA1207, doi:10.1029/2006PA001298.

Langer, M. (2008), Assessing the contribution of foraminiferan protists to global ocean carbonate production, *J. Eukaryot. Microbiol.*, *55*(3), 163–169.

Lohmann, G. P. (1995), A model for variation in the chemistry of planktonic foraminifera due to secondary calcification and selective dissolution, *Paleoceanography*, *10*(3), 445–457.

Mangerud, J., and S. Gulliksen (1975), Apparent radiocarbon ages of recent marine shells from Norway Spitsbergen, and Arctic Canada, *Quat. Res.*, *5*, 263–273.

Manley, T. O. (1995), Branching of Atlantic Water within the Greenland-Spitsbergen passage: An estimate of recirculation, *J. Geophys. Res.*, *100*(C10), 20,627–20,634.

Marnela, M., B. Rudels, K. A. Olsson, L. G. Anderson, E. Jeansson, D. J. Torres, M. J. Messias, J. H. Swift, and A. Watson (2008), Transports of Nordic Seas water masses and excess SF_6 through Fram Strait to the Arctic Ocean, *Prog. Oceanogr.*, *78*(1), 1–11, doi:10.1016/j.pocean.2007.06.004.

Martinson, D. G., N. G. Pisias, J. D. Hays, J. Imbrie, T. C. Moore, and J. Shackleton (1987), Age dating and the orbital theory of the Ice Ages: Development of a high-resolution 0 to 300,000-yr chronostratigraphy, *Quatern. Res.*, *27*, 1–29.

McManus, J. F., R. Francois, J. M. Gherardi, L. D. Keigwin, and S. Brown-Leger (2004), Collapse and rapid resumption of Atlantic meridional circulation linked to deglacial climate changes, *Nature*, *428*, 834–837, doi:10.1038/nature02494.

Mix, A. E., E. Bard, and R. Schneider (2001), Environmental processes of the ice age: land, ocean, glaciers (EPILOG), *Quat. Sci. Rev.*, *20*, 627–657, doi:10.1016/S0277-3791(00)00145-1.

Müller, J., G. Massé, R. Stein, and S. T. Belt (2009), Variability of sea-ice conditions it the Fram Strait over the past 30,000 years, *Nat. Geosci.*, doi:10.1038/NGEO665.

Nørgaard-Pedersen, N., R. F. Spielhagen, H. Erlenkeuser, P. M. Grootes, J. Heinemeier, and J. Knies (2003), Arctic Ocean during the last glacial maximum: Atlantic and polar domains of surface water mass distribution and ice cover, *Paleoceanography*, *18*, 1063, doi:10.1029/2002PA000781.

Peck, V. L., I. R. Hall, R. Zahn, H. Elderfield, F. Grousset, S. R. Hemming, and J. D. Scourse (2006), High resolution evidence for linkages between NW European ice sheet instability and Atlantic meridional overturning circulation, *Earth Planet. Sci. Lett.*, *243*, 476–488.

Peck, V. L., I. R. Hall, R. Zahn, and H. Elderfield (2008), Millennial-scale surface and subsurface paleothermometry from the northeast Atlantic, 55–8 ka BP, *Paleoceanography*, *23*, PA3221, doi:10.1029/2008PA001631.

Pflaumann, U., et al. (2003), Glacial north Atlantic: sea-surface conditions reconstructed by GLAMAP 2000, *Paleoceanography*, *18*(3), 1065, doi:10.1029/2002PA000774.

Rasmussen, T. L., and E. Thomsen (2008), Warm Atlantic surface water inflow to the Nordic seas 34–10 calibrated ka B.P., *Paleoceanography*, *23*, PA1201, doi:10.1029/2007PA001453.

Rasmussen, T. L., T. C. E. van Weering, and L. Labeyrie (1997), Climatic instability, ice sheets and ocean dynamics at high northern latitudes during the Last Glacial period (58–10 ka BP), *Quat. Sci. Rev.*, *16*, 71–80.

Rasmussen, T. L., E. Thomsen, M. A. Ślubowska, S. Jessen, A. Solheim, and N. Koç (2007), Paleoceanographic evolution of the SW Svalbard margin (76°N) since 20,000 ^{14}C yr BP, *Quat. Res.*, *67*(1), 100–114, doi:10.1016/j.yqres.2006.07.002.

Sanyal, A., N. G. Hemming, G. N. Hanson, and W. S. Broecker (1995), Evidence for a higher pH in the glacial ocean from boron isotopes in foraminifera, *Nature*, *373*, 234–236.

Sarnthein, M., U. Pflaumann, and M. Weinelt (2003), Past extent of sea ice in the northern North Atlantic inferred from foraminiferal paleotemperature estimates, *Paleoceanography*, *18*(2), 1047, doi:10.1029/2002PA000771.

Schiebel, R. (2002), Planktic foraminiferal sedimentation and the marine calcite budget, *Global Biogeochem. Cycles*, *16*(4), 1065, doi:10.1029/2001GB001459.

Schiebel, R., S. Barker, R. Lent, and H. Thomas (2007), Planktic foraminiferal dissolution in the twilight zone, *Deep Sea Res., Part II*, *54*, 676–686, doi:10.1016/j.dsr2.2007.01.009.

Scott, D. B., T. Schell, A. Rochon, and S. Blasco (2008), Modern benthic foraminifera in the surface sediments of the Beaufort shelf, slope and Mackenzie trough, Beaufort Sea, Canada: Distributions and taxonomy, *J. Foraminiferal Res.*, *38*, 228–250, doi:10.2113/gsjfr.38.3.228.

Scourse, J. D., A. I. Haapaniemi, E. Colmenero-Hidalgo, V. L. Peck, I. R. Hall, W. E. N. Austin, P. C. Knutz, and R. Zahn (2009), Initiation, dynamics, and deglaciation of the last British-Irish Ice Sheet: The deep-sea ice-rafted detritus record, *Quat. Sci. Rev.*, *28*, 3066–3084, doi:10.1016/j.quascirev.2009.08.009.

Sigman, D. M., and E. A. Boyle (2000), Glacial/interglacial variations in atmospheric carbon dioxide, *Nature*, *407*, 859–869.

Sigman, D. M., M. P. Hain, and G. H. Haug (2010), The polar ocean and glacial cycles in atmospheric CO_2 concentration, *Nature*, *466*, 47–55.

Simstich, J., M. Sarnthein, and H. Erlenkeuser (2003), Paired delta ^{18}O signals of *Neogloboquadrina pachyderma* (s) and *Turborotalita quinqueloba* show thermal stratification structure in Nordic Seas, *Mar. Micropaleontol.*, *48*(1–2), 107–125, doi:10.1016/S0377-8398(02)00165-2.

Smith, W. O., Jr., and E. Sakshaug (1990), Polar phytoplankton, 477–525, in *Polar Oceanography*, *Part B*, *Chemistry*, *Biology and Geology*, edited by W. O. Smith Jr., pp. 477–525 , Academic Press, New York.

Stanford, J. D., E. J. Rohling, S. Bacon, A. P. Roberts, F. E. Grousset, and M. Bolshaw (2011), A new concept for the paleoceanographic evolution of Heinrich event 1 in the North Atlantic, *Quat. Sci. Rev.*, *30*, 1047–1066, doi:10.1016/j.quascirev.2011.02.003.

Swift, J. H., and K. Aagaard (1981), Seasonal transitions and water mass formation in the Iceland and Greenland Sea, *Deep-Sea Research*, *28*, 1107–1129.

Vinje, T. E. (1977), Sea ice conditions in the European sector of the marginal seas of the Arctic, 1966–75, *Norw. Polar Inst.*, *1975*, 163–174.

Walczowski, W., J. Piechura, R. Osiński, and P. Wieczorek (2005), The West Spitsbergen Current volume and heat transport from synoptic observations in summer, *Deep Sea Res., Part I*, *52*(8), 1374–1391, doi:10.1016/j.dsr.2005.03.009.

Weinelt, M., E. Vogelsang, M. Kucera, U. Pflaumann, M. Sarnthein, A. Voelker, H. Erlenkeuser, and B. A. Malmgren (2003),Variability of North Atlantic heat transfer during MIS 2, *Paleoceanography*, *18*(3), 1071, doi:10.1029/2002PA000772.

Werner, K., R. F. Spielhagen, D. Bauch, H. C. Hass, and E. Kandiano (2013), Atlantic Water advection versus sea-ice advances in the eastern Fram Strait during the last 9 ka: Multiproxy evidence for a two-phase Holocene, *Paleoceanography*, *28*, 283–295, doi:10.1002/palo.20028.

Wollenburg, J. E., J. Knies, and A. Mackensen (2004), High-resolution paleoproductivity fluctuations during the past 24 kyr as indicated by benthic foraminifera in the marginal Arctic Ocean, *Palaeogeogr. Palaeoclimatol. Palaeoecol.*, *204*, 209–238.

Yokoyama, Y., K. Lambeck, P. De Deckker, P. Johnston, and L. K. Fifield (2000), Timing of the Last Glacial Maximum from observed sea level minima, *Nature*, *406*, 713–716.

Zamelczyk, K., T. L. Rasmussen, K. Husum, H. Haflidason, A. de Vernal, E. K. Ravna, M. Hald, and C. Hillaire-Marcel (2012), Paleoceanographic changes and calcium carbonate dissolution in the central Fram Strait during the last 20 ka yr, *Quat. Res.*, *78*, 405–416, doi:10.1016/j.yqres.2012.07.006.

Zamelczyk, K., T. L. Rasmussen, K. Husum, and M. Hald (2013), Marine calcium carbonate preservation vs. climate change over the last two millennia in the Fram Strait: Implications for planktic foraminiferal paleostudies, *Mar. Micropaleontol.*, *98*, doi:10.1016/j.marmicro.2012.10.001.